Available online at www.sciencedirect.com
ScienceDirect
Dyes and Pigments 76 (2008) 784–791
DYES and PIGMENTS
www.elsevier.com/locate/dyepig

Adsorption of binary mixtures of cationic dyes

B. Noroozi [a,b], G.A. Sorial [a,*], H. Bahrami [b], M. Arami [b]

[a] Department of Civil and Environmental Engineering, University of Cincinnati, P.O. Box 210071, Cincinnati, OH 45221-0071, USA
[b] Textile Engineering Department, Amirkabir University of Technology, Tehran, Iran

Received 17 December 2006; received in revised form 1 February 2007; accepted 7 February 2007
Available online 20 February 2007

Abstract

Adsorption of cationic textile dyes namely, C.I. Basic Blue 41 and C.I. Basic Red 18 onto granular activated carbon (GAC) and silkworm pupa (SWP – a natural adsorbent) has been investigated for single and binary solute systems. Equilibrium isotherms were conducted for two, single solute systems and three binary combinations of the dyes. Although adsorption of C.I. Basic Red 18 on SWP showed no correlation with the Langmuir, Freundlich or Myers models, the Freundlich equation described the adsorption of Basic Blue 41 well and the Myers equation correlated reasonably well the two dyes on GAC. Of the multi-component models studied, the ideal adsorbed solution theory (IAST) gave reasonable predictions of the binary systems of the dyes on GAC but it failed to predict the binary system on SWP. The adsorption on SWP was shown to occur by chemisorption which was not affected by the presence of molecular oxygen.

Keywords: C.I. Basic Blue 41; C.I. Basic Red 18; Granular activated carbon (GAC); Ideal adsorbed solution theory (IAST); Multi-component isotherms; Silkworm pupa

1. Introduction

Textile Industries consume large volumes of water and chemicals. Wastewater streams from the textile dyeing operation contain unused dyes (about 8–20% of the total pollution load due to incomplete exhaustion of the dye) and auxiliary chemicals along with large amounts of water [1]. The presence of dyes in water sources is aesthetically unacceptable and may be visible at concentration as low as 1 ppm [2]. Such waste streams require treatment [1]; conventional methods for the removal of dyes from wastewater include adsorption onto solid substrates, chemical coagulation, disinfection, filtration and UV treatment. Adsorption has become a well-established separation technique to remove dilute pollutants as well as offering the potential for regeneration, recovery and recycling of the adsorbed materials [3]. Adsorption is a physico-chemical wastewater treatment process that is gaining prominence as a means of producing high quality effluent that is low in dissolved organic compounds. The important characteristics of an adsorbent are described in terms of both adsorptive capacity and physical properties [4].

Equilibrium adsorption isotherms play an important role in the predictive modelling that is used for the analysis and design of adsorption systems. As such models can be used to predict the performance of an adsorption process under a range of operating conditions, adsorption isotherms are invaluable tools for theoretical evaluation. However, no single model has been found to be generally applicable because although one isotherm equation may fit experimental data accurately under one set of conditions, it may fail entirely under another [5]. Although considerable information has been collected for the adsorption of single component dyes by various adsorbents, many industrial situations involve the discharge of effluents that contain a mixture of several dyes [6]; limited data is available on multi-component dye adsorption. The study of multi-component adsorption presents a major challenge compared to single component adsorption mainly due to the increased complexity brought about by the increasing number of parameters needed for process description. The various possible interactions and

* Corresponding author. Tel.: +1 5135562987; fax: +1 5135562599.
E-mail address: george.sorial@uc.edu (G.A. Sorial).

0143-7208/$ - see front matter © 2007 Elsevier Ltd. All rights reserved.
doi:10.1016/j.dyepig.2007.02.003

Nomenclature

a_L^0	Langmuir isotherm constant (l/mmol)
BB41	Basic Blue 41
BR18	Basic Red 18
C_e	concentration of adsorbate at equilibrium (mmol/l)
C_i	initial concentration of the adsorbate (mmol/l)
GAC	granular activated carbon
H	Myers isotherm regression parameter (l/g)
HPLC	high performance liquid chromatography
IAST	ideal adsorbed solution theory
K	Myers isotherm regression parameter ($(mmol/g)^{-p}$)
K_f	Freundlich isotherm constant ($(mmol/g)/(mmol/l)^n$)
K_L^0	Langmuir isotherm constant (l/g)
m	dry weight of adsorbent (g)
n	Freundlich isotherm constant
p	Myers isotherm regression parameter
pH_{pzc}	pH of the point of zero charge
q_e	amount of solute adsorbed at equilibrium (mmol/g)
Q_i	capacity of adsorbent for component i in a multi-component system (mmol/g)
Q_m^0	monolayer saturation capacity for the single solute Langmuir isotherm (mmol/g)
Q_T	total capacity of the adsorbent in multi-component system (mmol/g)
SSRE	sum of squares of relative error
SWP	silkworm pupa
V	volume of solution used in the adsorption experiment (l)

competition between adsorbates and adsorbent in a multi-component system complicate the adsorption process. However, an efficient, accurate and cost effective design should account for multi-component adsorption [7]. Prediction of the equilibrium adsorption of mixtures from pure-component isotherms is important for practical application [8].

Activated carbon is the most popular adsorbent used in wastewater treatment and in the removal of dyes. Several equilibrium studies on the adsorption of dyes using activated carbon and its derivatives have been carried out [9–12]. Some authors have investigated multi-component dye systems based on activated carbon and peat [3,5,10,13,14]. Over the last decade, the low cost and commercial availability of biosorbents have stimulated great attention into the possibility of using various low cost adsorbents [15–18]. However, almost all of these studies were based on single solute systems due to complications in the adsorption mechanisms of natural adsorbents. However, the use of such materials as adsorbents will be important if studies are conducted for multi-component systems.

This work concerns the single and binary adsorption of two cationic dyes, C.I. Basic Blue 41 (BB41) and C.I. Basic Red 18 (BR18) by SWP (a residue obtained during silk yarn processing) as a natural adsorbent and granular activated carbon (GAC) as a popular adsorbent. The single component adsorption was modeled using the Langmuir, Freundlich and Myers isotherms. Extensions of the Langmuir equation, the Jain and Snoeyink modified extended Langmuir (JS extended Langmuir) model and ideal adsorbed solution theory (IAST) were used to model the experimental binary data.

2. Materials and methods

2.1. Dyes

BB41 dye was purchased from Sigma–Aldrich, and BR18 dye was obtained from Ciba, Iran. Table 1 and Fig. 1 show the properties and structures of the dyes, respectively. Stock aqueous solutions (1000 mg/l) of the dyes were prepared in autoclaved deionized water.

2.2. Preparation of adsorbent

F400 (Filtrasorb 400; Calgon, Pittsburg, PA) was used as a typical GAC. SWP, obtained from Pileh va Abrisham Shomal Co., Rasht, Iran, was washed with distilled water, dried and ground. The powdered pupa was then sieved (50–100 mesh) and used as adsorbent. The general analysis of SWP showed that it contained 58% protein, 24% minerals, 8% fat, 5% water and 5% ash. Both the SWP and the GAC adsorbents were dried at 110 °C overnight to remove moisture and were stored in a desiccator until use. The physical properties of GAC F400 and SWP were determined by conducting nitrogen adsorption at 77.2 K for determining the multipoint specific surface area and the basic t-plot micropore analysis using a TriStar 3000 gas adsorption analyzer.

2.3. Methods

The bottle point method, which is described below, was used at 22 ± 1 °C for the adsorption studies. Three initial concentrations with different adsorbent masses were used for the single solute systems. A weighed quantity of adsorbent was placed in a bottle (125 ml) containing 100 ml of a dye solution. The mass of SWP ranged from 10 to 180 mg/bottle, 12 to 240 mg/bottle and 15 to 280 mg/bottle for initial dye concentrations of 0.1, 0.2 and 0.4 mmol/l, respectively. The mass of GAC ranged from 1 to 10 mg/bottle, 6 to 26 mg/bottle and 10 to 30 mg/bottle for initial dye concentrations of 0.1, 0.2 and 0.4 mmol/l, respectively. The pH of the adsorbent–adsorbate

Table 1
Properties of the studied dyes

Characteristics	Dye	
	BB41	BR18
C.I. name	Basic Blue 41	Basic Red 18
Chemical structure	Mono-azo	Mono-azo
M_w (g/mol)	483	391
λ_{max} (nm)	610	480

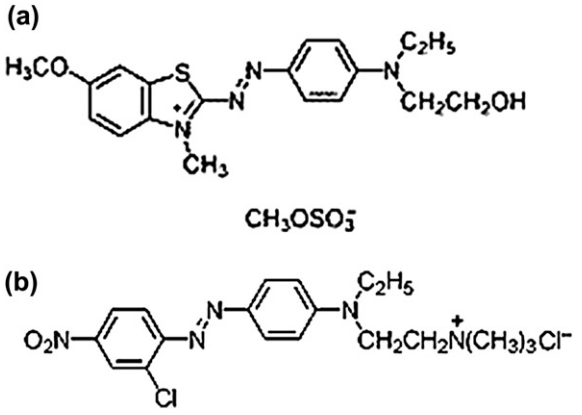

Fig. 1. Structure of the dyes: (a) BB41 and (b) BR18.

system was buffered to 7 using potassium dihydrogen phosphate and sodium hydroxide. The bottles were sealed and rotated for two weeks using a horizontal shaker at 150 rpm. To eliminate any change in the nature of dye solution during the experiment, two bottles for each concentration with no adsorbent present were also used. The λ_{max} of the dyes was determined using a Shimadzu UVmini 1240 UV–vis spectrophotometer; after equilibration, solutions were filtered through 0.1 μm nylon filters (Micron Separation, Inc) prior to analysis in order to minimize interference of the adsorbent fines with the analysis. The first 15 ml of the filtered sample was discarded in order to minimize the impact of potential adsorption of the adsorbate on the filter membrane. Concentrations were measured using an Agilent 1100 Series HPLC equiped with a diode array detector; analysis was performed on a reversed phase Supelco LC18 column (15 cm × 4.6 mm, 5 μm). The mobile phase comprised 50% acetonitrile and 50% water for BB41 and 50% methanol and 50% water for BR18 with a flow rate of 0.8 ml/min and a post-time of 4 min for BB41 and 10 min for BR18; the temperature of the column was maintained at 30 °C. The equilibrium concentration of each solution was determined by interpolation with the calibration curve at the λ_{max} of the dye, namely 610 nm for BB41 and 480 nm for BR18.

The isotherm procedure mentioned above was also used for the binary solute system (BB41/BR18). Three concentration combinations of the dyes were used. The range of the concentrations for BB41 and BR18 were 0.2–0.5 mmol/l and 0.2–0.4 mmol/l, respectively. The range of masses of adsorbents employed for binary systems ranged from 3 to 50 mg/bottle and 14 to 330 mg/bottle for GAC and SWP, respectively.

For the anoxic isotherms, accurately weighed masses of SWP were placed in 125-ml glass-amber bottles and the adsorbent was then purged with high-purity nitrogen to remove molecular oxygen. The different dye solutions were prepared in autoclaved deionized water buffered with KH_2PO_4 and the pH was adjusted to 7.0 in a 4-l bottle. Before adding the dyes to the 4-l bottle, dissolved oxygen in the buffered water was eliminated by stripping the water with high-purity nitrogen for 3 h. The dyes in powder form were then added and the ensuing solution was mixed for 1 h. The 4-l bottle was then kept under nitrogen to eliminate the presence of oxygen in the headspace.

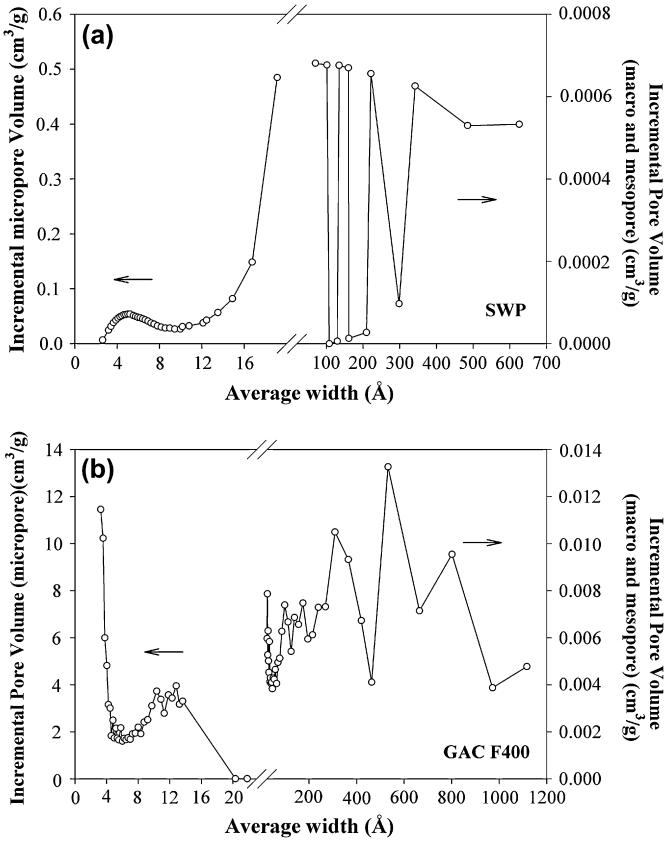

Fig. 2. Pore size distribution of (a) SWP and (b) GAC F400.

The 125-ml glass-amber bottles containing the different masses of SWP were then completely filled with the dye solutions, sealed tightly with Teflon lined caps and covered by Parafilm.

3. Results and discussion

3.1. Properties of the adsorbents

Nitrogen adsorption at 77.2 K was used to determine multipoint specific surface and basic *t*-plot micropore analysis. The pore size distribution of the two adsorbents is shown in Fig. 2 from which it is evident that F400 had a wide pore size distribution ranging from 4 to 800 Å. Although the maximum N_2 adsorption by SWP occurred in pores ranging between 4 and 20 Å, no significant porosity was found. Furthermore, as the amount of N_2 adsorbed was very small compared to GAC, SWP can be considered as a non-porous material (Table 2).

Table 2
Physical properties of GAC and SWP

Property	GAC F400	SWP
BET surface area (m^2/g)	992.98	0.1730
Micropore area (m^2/g)	892.93	–
External surface area (m^2/g)	100.05	0.1988
BJH adsorption average pore diameter (Å)	46.255	465.345
Micropore volume (cm^3/g)	0.373	–
Total pore volume (cm^3/g)	0.615	0.000750
Fraction microporosity (%)	60.7	–

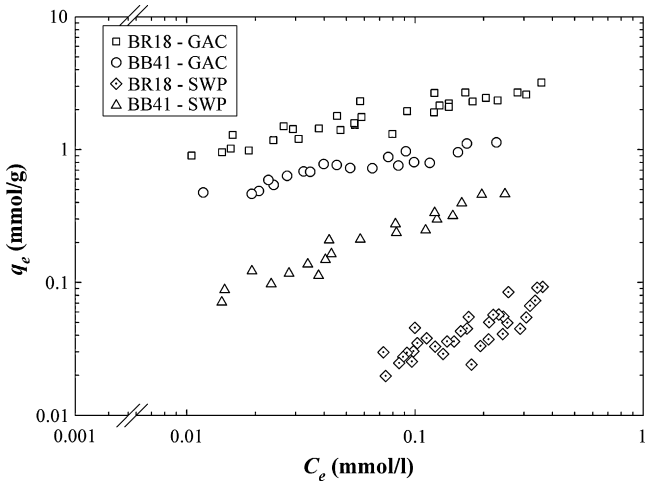

Fig. 3. Single solute adsorption isotherm of cationic dyes.

The pH at the point of zero charge, pH_{pzc} (i.e., the pH above which the total surface of the adsorbent particles is negatively charged) was measured for both GAC and SWP, by the so-called pH drift method [19]. The results indicated that the pH_{pzc} was 5.8 and 9.8 for SWP and GAC, respectively. Despite the different pH_{pzc} for both adsorbents, all experiments were conducted at pH 7 in order to ensure stability of both dyes (the dyes dissociate at a pH > 9.5).

3.2. Single solute equilibrium studies

The experimental equilibrium adsorption data at 22 °C are represented in Fig. 3. Equilibrium surface loading, q_e, was calculated from the mass balance equation around the isotherm bottle:

$$q_e = \frac{V(C_i - C_e)}{m} \tag{1}$$

where V is the volume of solution used in the adsorption experiment, C_i and C_e are the initial and equilibrium concentrations of the adsorbate (mmol/l), respectively, and m is the dry mass of the adsorbent (g).

Fig. 3 clearly indicates that there was a significant difference between the adsorption capacity of GAC and SWP for BB41 and BR18. The data in Fig. 3 were then compared using three adsorption isotherm models.

(i) The Langmuir [20] isotherm equation is given by

$$q_e = \frac{K_L^0 C_e}{1 + a_L^0 C_e} \tag{2}$$

where C_e is the concentration of adsorbate (mmol/l) at equilibrium, q_e is amount of solute adsorbed at equilibrium (mmol/g), K_L^0 (l/g) and a_L^0 (l/mmol) are constants.

(ii) The Freundlich [21] isotherm equation is given by

$$q_e = K_f C_e^n \tag{3}$$

where q_e is amount of adsorbate at equilibrium (mmol/g), C_e is the adsorbate concentration in the solution (mmol/l) at equilibrium and K_f and n are constants incorporating all factors affecting the adsorption process such as adsorption capacity and intensity.

(iii) The Myers [22] isotherm equation is given by

$$C_e = \frac{q_e}{H} \exp\left(K q_e^p\right) \tag{4}$$

where C_e is the liquid-phase concentration (mmol/l), q_e is surface loading (mmol/g), H, K and p are regression parameters.

The corresponding parameters in each equation were determined using linear regression analysis. The sum of squares of relative error (SSRE) was calculated by Eq. (5).

$$\text{SSRE} = \sum \left(\frac{q_{e,i}\text{observed} - q_{e,i}\text{predicted}}{q_{e,i}\text{observed}} \right)^2 \tag{5}$$

Table 3 presents the parameters obtained together with the SSRE values from which it is apparent that the BR18-SWP

Table 3
Regression parameters for the single solute isotherm equations

Isotherm	Parameter	Adsorbent			
		GAC		SWP	
		BB41	BR18	BB41	BR18
Langmuir	K_L (l/g)	58.82	116.27	6.33	0.42
	a (l/mmol)	57.95	60.53	13.46	4.17
	SSRE[a]	0.200	0.453	0.515	2.028
Freundlich	K_f (mmol/g)/(mmol/l)^n	1.752	4.191	1.169	0.137
	n	0.298	0.326	0.629	0.665
	SSRE	0.161	0.454	0.332	1.883
Myers	H (l/g)	$8.54 \times 10^{+9}$	$4.39 \times 10^{+5}$	$5.78 \times 10^{+5}$	4.063
	K (mmol/g)$^{-p}$	20.99	8.67	12.49	4.31
	p	1.15×10^{-1}	1.99×10^{-1}	4.99×10^{-2}	1.94×10^{-1}
	SSRE	0.109	0.121	2.983	2.431

[a] SSRE: sum of squares of relative error.

Table 4
Recovery efficiency of the dyes from used adsorbents

Dye	SWP		GAC	
	Adsorbed dye (mmol/g)	Recovered dye (%)	Adsorbed dye (mmol/g)	Recovered dye (%)
BB41	0.521	20.2	2.407	91.4
	0.282	16.4	1.456	89.1
	0.178	37.4	1.178	86.6
BR18	0.137	21.2	3.231	96.5
	0.093	24.1	2.492	90.4
	0.075	6.1	2.251	85.2

adsorption system provided no desirable SSRE value, i.e., >1. The adsorption of BR18 on GAC showed good agreement with the Myers equation while the Freundlich isotherm model was found to be the best to describe BB41 adsorption on SWP; adsorption of BB41 on GAC gave the lowest SSRE value of the three isotherm models.

The molecular characteristics of dyes and the physico-chemical properties of an adsorbent can affect adsorption. In order to determine the adsorption mechanism, adsorbent samples were extracted after equilibration with the dyes using methanol for 1 day followed by 3 days of extraction with dichloromethane. The recovery efficiency of the adsorbents after adsorption (see Table 4) confirmed that the predominant adsorption mechanisms were chemisorption for SWP and physisorption for GAC. The tendency for physisorption to occur in the case of SWP was limited due to its non-porosity. Experimental results further revealed that chemisorption in the case of BB41 was non-destructive as compared to BR18. On comparing the UV–vis and HPLC measurements of BR18 adsorption onto SWP, significant differences were found. HPLC analysis showed that only a small amount of the dye had been adsorbed, whereas UV–vis spectroscopy showed large dye removal. This discrepancy between the two techniques can be attributed to the fact that the colour of the solution was reduced while the dye molecule remained in solution. It is proposed that the amino-acid nature of the SWP may have provided redox reactions that decolourised the dye during the adsorption process. This was revealed by exposing SWP to the oxidants potassium permanganate and sodium hypochlorite.

3.3. Binary solute equilibrium studies

Adsorption isotherms for the binary system of the two dyes were conducted for the three initial concentrations listed in Table 5. By measuring the concentration of the individual dye after equilibrium, the surface loading, q_e, was calculated using mass balance (Eq. (1)). The equilibrium adsorption data were then analyzed by various multi-component models namely, the extended Langmuir, JS extended Langmuir and IAST equations. Evaluation of each model was done by calculating the SSRE (Table 5).

For multi-component systems, adsorbent–adsorbate affinity will change due to competition for available adsorption sites. Different molecular species interact differently in solution and on the adsorbent surface, leading to a different loading Q_i (capacity of adsorbent for component i in a multi-component system) and Q_T (total capacity of the adsorbent in multi-component system) [23], where:

$$Q_T = \sum_{i=1}^{n} Q_i \tag{6}$$

and n is the number of components.

The above effects act together to produce a new adsorption system. Butler and Ockrent [24] developed the Langmuir model for competitive adsorption which assumed (i) a homogeneous surface with respect to the energy of adsorption, (ii) no interaction between adsorbed species, and (iii) that all adsorption sites were equally available to all adsorbed species [6] (Eq. (7))

$$q_{e,i} = \frac{K^0_{L,i} C_{e,i}}{1 + \sum a^0_{L,i} C_{e,i}} \tag{7}$$

Table 5
SSRE value of applied models for binary systems

Adsorbent	Run	Initial dye concentrations (mmol/l)	SSRE[a]					
			IAST		Extended Langmuir		JS extended Langmuir	
			BB41	BR18	BB41	BR18	BB41	BR18
GAC	1	BB41: 0.51 BR18: 0.20	0.054	0.066	0.033	4.286	0.033	0.289
	2	BB41: 0.41 BR18: 0.35	0.039	0.084	0.268	3.023	0.268	0.322
	3	BB41: 0.21 BR18: 0.38	0.146	0.114	0.857	1.776	0.857	0.592
SWP	4	BB41: 0.49 BR18: 0.20	42.79	1.043	2.912	1.772	3.713	1.772
	5	BB41: 0.49 BR18: 0.39	149.91	1.253	14.26	2.414	24.57	2.414
	6	BB41: 0.22 BR18: 0.39	4.064	0.275	0.647	0.564	0.711	0.564

[a] SSRE: sum of squares of relative error.

where $K^0_{L,i}$ and $a^0_{L,i}$ are the Langmuir isotherm constants obtained from the single solute system.

Table 5 shows that the extended Langmuir model provided poor prediction insofar as the SSRE values were relatively high. BB41 showed a reasonable SSRE value for concentration combinations where the amount of BB41 was significantly higher than BR18 (i.e., run 1 for GAC). According to Table 5, in the case of the adsorption of BB41 on GAC, the SSRE value increased with increasing initial molar ratio of BR18:BB41, this contrasting with the result obtained for the adsorption of BR18 on GAC. Implicit assumptions in the extended Langmuir model indicate that the adsorbates in multi-component mixture behave independently, i.e., there are no competition, interaction or displacement effects. However, this is not attained in multi-component mixtures as there is significant interaction and competition occurring.

Jain and Snoeyink [25] investigated the competitive adsorption on activated carbon of aqueous binary solutions of organic adsorbates and developed a model that predicted adsorption equilibrium for non-ideal systems. The resulting JS extended Langmuir model adds an additional term to the extended Langmuir equation (Eqs. (8) and (9)) [6].

$$q_{e,1} = \frac{\left(Q^0_{m,1} - Q^0_{m,2}\right) a^0_{L,1} C_{e,1}}{1 + a^0_{L,1} C_{e,1}} + \frac{Q^0_{m,2} a^0_{L,1} C_{e,1}}{1 + a^0_{L,1} C_{e,1} + a^0_{L,2} C_{e,2}} \quad (8)$$

$$q_{e,2} = \frac{Q^0_{m,2} a^0_{L,2} C_{e,2}}{1 + a^0_{L,1} C_{e,1} + a^0_{L,2} C_{e,2}} \quad (9)$$

where Q^0_m is the monolayer saturation capacity for the single solute Langmuir isotherm (mmol/g). This model was found to be valid for binary systems with large molecular size differences or chemical properties with respect to the adsorbent; however, for more than two components this model failed to provide good predictions [26]. The SSRE values reported in Table 5 for the JS extended Langmuir model clearly indicate an improvement in prediction for BR18 on GAC compared to the extended Langmuir model. In the case of SWP, no significant changes were noticed; furthermore, the SSRE values of both dyes on GAC increased with increasing initial molar ratio of BR18:BB41.

The model with the most thermodynamically accepted foundation is the IAST, which was originally proposed by Myers and Prausnitz [27] for gas mixtures and later developed for dilute liquid solutions. The IAST theory provides a thermodynamically consistent and practical method for predicting binary adsorption isotherms using single solute isotherm data alone. In this paper, the adsorption data for the binary systems were tested against IAST predictions using Myers equation parameters obtained from the single solute dye systems (Table 3). The basis of the theory has been demonstrated by Lu and Sorial [28].

Figs. 4 and 5 compare the experimental data and prediction using IAST for the binary adsorption of BB41 and BR18 on GAC and SWP. As shown in Table 5, IAST provides best prediction for the binary adsorption system on GAC with the lowest values of SSRE (<0.15). It can be seen from Fig. 4 that for all binary systems, the amount of BR18 adsorbed onto GAC was higher than that of BB41. From Fig. 1 and Table 1 it is apparent that the M_w and molecular size of BB41 are greater than BR18, hence, when in competition, the smaller molecule will occupy the pores in the GAC first. For systems where the predominant adsorption mechanism is chemisorption, the role of

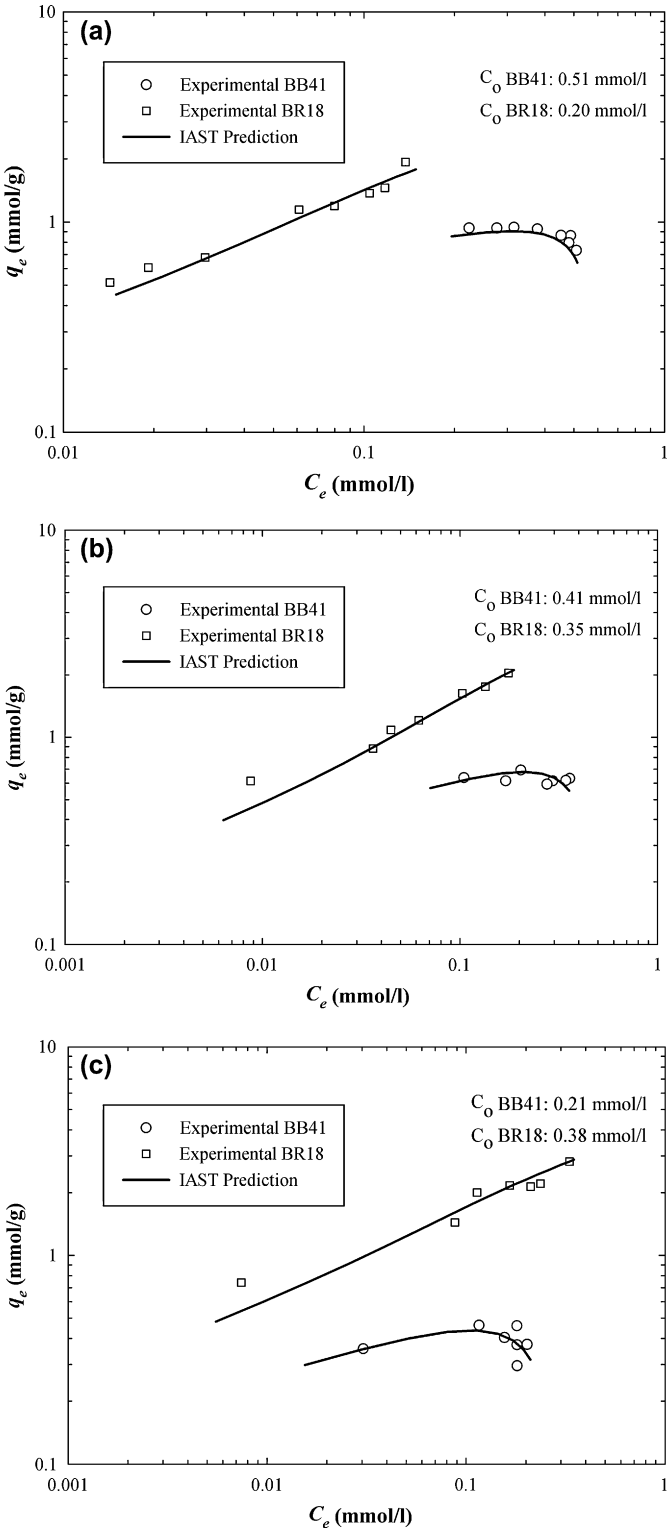

Fig. 4. IAST prediction of binary adsorption of cationic dyes on GAC.

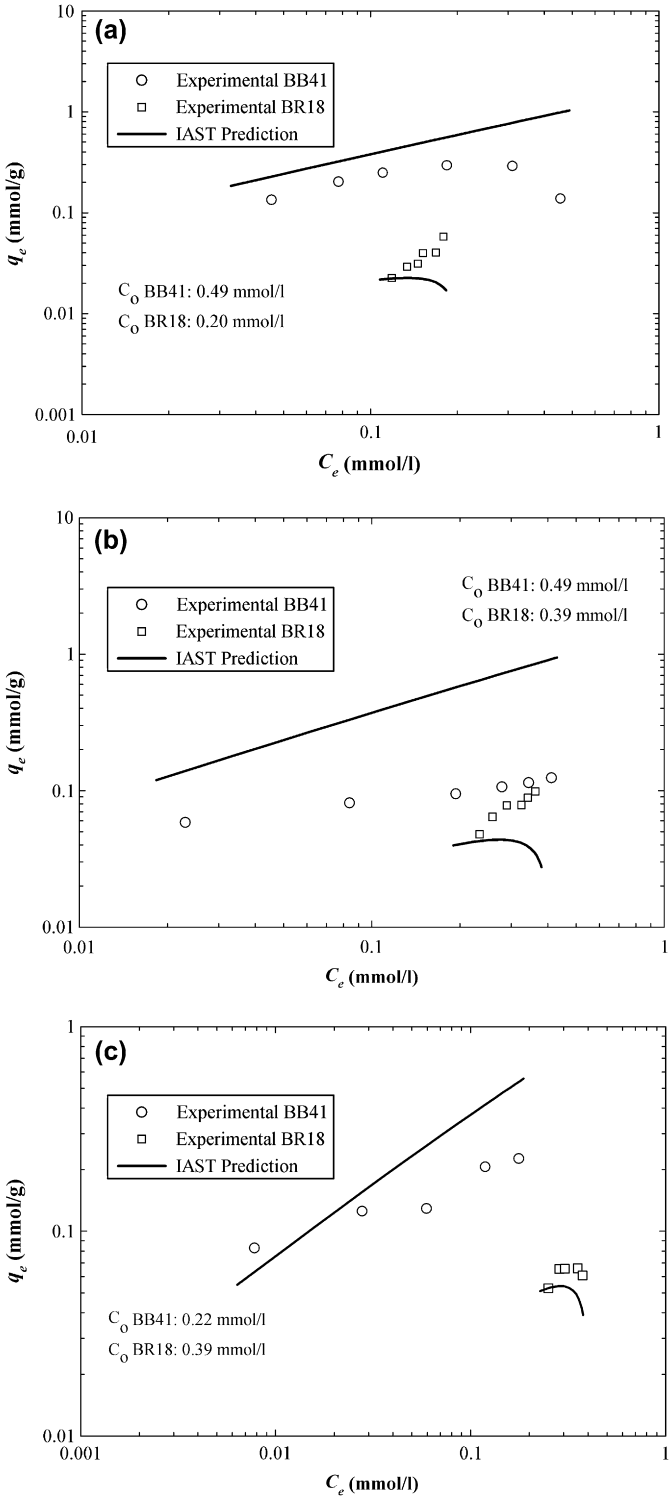

Fig. 5. IAST prediction of binary adsorption of cationic dyes on SWP.

molecular size will not play a major role. On comparing the structures of BB41 and BR18, one finds that the positive charge in BR18 is outside the aromatic rings and there are also two nitrogen atoms in BR18 which can be positively charged and interact with the surface of the adsorbent. It is worthwhile to note that the positive nitrogen in BB41 lies within the aromatic structure, and the presence of an electronegative atom, such

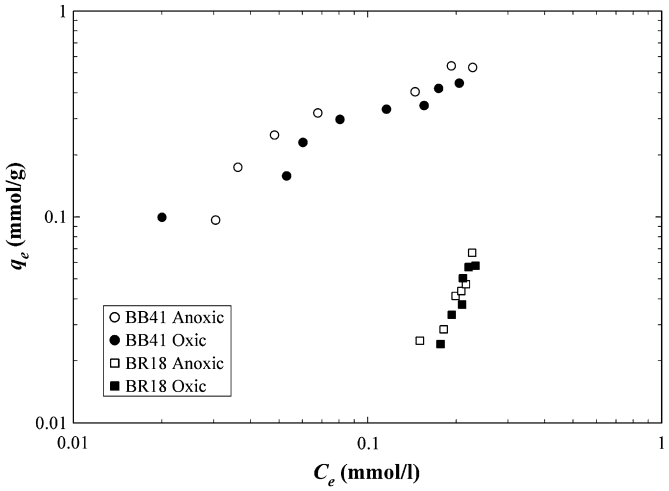

Fig. 6. Anoxic single solute adsorption of cationic dyes on SWP.

as sulfur, reinforces the positive charge on the dye molecule. The results obtained confirm that the adsorption of BB41 on SWP in both single and binary systems was higher than BR18. According to Table 5 and Fig. 5, IAST does not adequately predict dye adsorption on SWP because the model can be only applied to adsorption systems in which the predominant adsorption mechanism is physisorption [28]. As discussed previously, adsorption of the dye by SWP was suspected to occur by chemisorption, and hence it is proposed that the presence of molecular oxygen during the adsorption process may have contributed to this chemisorption. For this reason, both single and binary adsorptions were carried out in the absence of molecular oxygen using the method mentioned in Section 2.3. The data in Figs. 6 and 7 indicate that there was no significant difference between the amount of BB41 and BR18 adsorbed on SWP under oxic (presence of molecular oxygen) and anoxic (absence of molecular oxygen) conditions (Fig. 6). Thus, it can be deduced that molecular oxygen does not impact SWP–cationic dye adsorption. Binary adsorption under anoxic condition demonstrated that IAST cannot predict

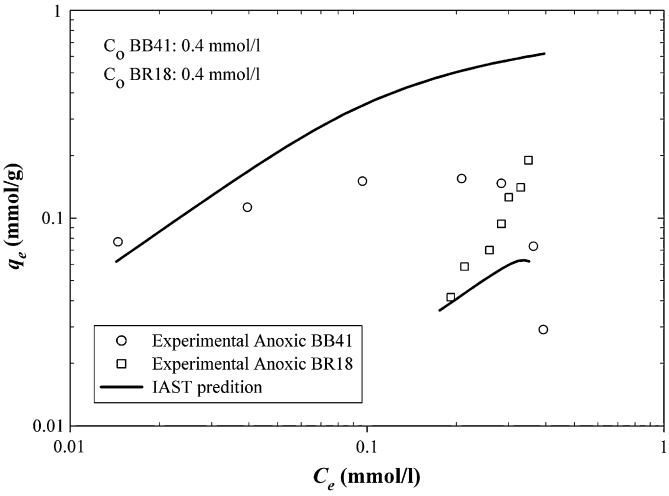

Fig. 7. Anoxic IAST prediction of binary adsorption of cationic dyes on SWP.

the adsorption of the cationic dyes on SWP (Fig. 7) because the chemisorption mechanism of the dyes does not depend on whether molecular oxygen was present. It is speculated that functional groups on the surface of SWP played the main role in adsorption of the dyes.

4. Conclusions

Single solute adsorption of BB41 and BR18 on GAC were well described by the Myers equation. The SSRE for binary adsorption on GAC showed that IAST was more accurate than the extended Langmuir and JS extended Langmuir models. Molecular oxygen had no impact on the adsorption of BB41 and BR18 on SWP. The main factor which affects the physisorption on GAC in binary systems is the dye's molecular size. In the case of SWP, the chemical properties of the adsorbate and adsorbent effect the process of adsorption.

Acknowledgements

The authors would like to thank Guilan University (Rasht–Iran) and Ministry of Science, Research and Technology (Tehran–Iran) for providing the opportunity to conduct research in USA. This work has been produced with the assistance and financial support of the Environmental Chemistry Lab in the Civil and Environmental Engineering Department at the University of Cincinnati (Cincinnati, USA).

References

[1] Mukherjee AK, Gupta B, Chowdhury SMS. Separation of dyes from cotton dyeing effluent using cationic polyelectrolytes. Am Dyest Rep 1999;(February):25–8.
[2] O'Mahony T, Guibal E, Tobin JM. Reactive dye biosorption by *rhizopus arrhizus* biomass. Enzyme Microb Technol 2002;31:456–63.
[3] Mckay G, Allen SJ, Porter JF. Adsorption isotherm models for basic dye adsorption by peat in single and binary component systems. J Colloid Interface Sci 2004;280:322–33.
[4] McKay G, Choy KKH, Porter JF. Single and multicomponent equilibrium studies for the adsorption of acidic dyes on carbon from effluents. Langmuir 2004;20:9646–56.
[5] Vinod VP, Anirudhan TS. Adsorption behaviour of basic dyes on the humic acid immobilized pillared clay. Water Air Soil Pollut 2003;150:193–217.
[6] McKay G, Choy KKH, Porter JF. Langmuir isotherm models applied to the multicomponent sorption of acid dyes from effluent onto activated carbon. J Chem Eng Data 2000;45:575–84.
[7] Pravat RJ, Jayanta KB, Sirshendu D. A generalized shrinking core model for multicomponent batch adsorption processes. Chem Eng J 2004;102:267–75.
[8] Bai R, Deng J, Yang RT. Improved multisite Langmuir model for mixture adsorption using multiregion adsorption theory. Langmuir 2003;19:2776–81.
[9] Attia AA, Girgis BS, Khedr SA. Capacity of activated carbon derived from pistachio shells by H_3PO_4 in the removal of dyes and phenolics. J Chem Technol Biotechnol 2003;78:611–9.
[10] McKay G, Porter JF, Choy KH. The prediction of sorption from a binary mixture of acidic dyes using single- and mixed-isotherm variants of the ideal adsorbed solute theory. Chem Eng Sci 1999;54:5863–85.
[11] Namasivayam C, Kavitha D. Removal of congo red from water by adsorption onto activated carbon prepared from coir pith, an agricultural solid waste. Dyes Pigments 2002;54:47–58.
[12] Thomas A, Yeh RY-L. Color removal from dye wastewaters by adsorption using powdered activated carbon: mass transfer studies. J Chem Technol Biotechnol 1995;63:48–54.
[13] Gutierrez M, Fuentes HR. Modeling adsorption in multicomponent systems using a Freundlich-type isotherm. J Contam Hydrol 1993;14:247–60.
[14] Mckay G, Al Duri B. Prediction of bisolute adsorption isotherms using single component data for dye adsorption onto carbon. Chem Eng Sci 1988;43:1133–42.
[15] Cestari AR, Vieira EFS, Santos AGP, Mota JA, Almeida VP. Adsorption of anionic dyes on chitosan beads. 1. The influence of the chemical structures of dyes and temperature on the adsorption kinetics. J Colloid Interface Sci 2004;280:380–6.
[16] Garg VK, Gupta R, Bala Yadav A, Kumar R. Dye removal from aqueous solution by adsorption on treated sawdust. Bioresour Technol 2003;89:121–4.
[17] Indra DM, Vimal CS, Nitin KA. Removal of orange-G and methyl violet dyes by adsorption onto bagasse fly ash: kinetic study and equilibrium isotherm analyses. Dyes Pigments 2006;69:210–23.
[18] Mittala A, Krishnana L, Gupta VK. Removal and recovery of malachite green from wastewater using an agricultural waste material, de-oiled soya. Sep Purif Technol 2005;43:125–33.
[19] Lopez-Ramon MV, Stoeckli F, Moreno-Castilla C, Carrasco-Marin F. On the characterization of acidic and basic surface sites on carbons by various techniques. Carbon 1999;37:1215–21.
[20] Langmuir I. The constitution and fundamental properties of solids and liquids. J Am Chem Soc 1916;38:2221–95.
[21] Freundlich HMF. Uber die adsorption in losungen. Z Phys Chem 1906;57:385–471.
[22] Sorial GA, Lu Q. The role of adsorbent pore size distribution in multicomponent adsorption on activated carbon. Carbon 2004;42:3133–42.
[23] Mckay G, Al Duri B. Simplified model for the equilibrium adsorption of dyes from mixtures using activated carbon. Chem Eng Process 1987;22:145–56.
[24] Butler JAV, Ockrent C. Studies in electrocapillarity. III. J Phys Chem 1930;34:2841–59.
[25] Jain JS, Snoeyink VL. Adsorption from bisolute systems on active carbon. J Water Pollut Control Fed 1973;45:2463–79.
[26] Mckay G, Al Duri B. Prediction of multicomponent adsorption equilibrium data using empirical correlations. Chem Eng J 1989;41:9–23.
[27] Myers AL, Prausnitz JM. Thermodynamics of mixed-gas adsorption. AIChE J 1965;11:121–7.
[28] Lu Q, Sorial GA. Adsorption of phenolics on activated carbon-impact of pore size and molecular oxygen. Chemosphere 2004;55:671–9.